NASA/TM-20210009633 AIAA–2016–4630

# Post-Test Inspection of NASA's Evolutionary Xenon Thruster Long-Duration Test Hardware: Discharge Chamber

*Rohit Shastry and George C. Soulas*
*Glenn Research Center, Cleveland, Ohio*

June 2021

# NASA STI Program . . . in Profile

Since its founding, NASA has been dedicated to the advancement of aeronautics and space science. The NASA Scientific and Technical Information (STI) Program plays a key part in helping NASA maintain this important role.

The NASA STI Program operates under the auspices of the Agency Chief Information Officer. It collects, organizes, provides for archiving, and disseminates NASA's STI. The NASA STI Program provides access to the NASA Technical Report Server—Registered (NTRS Reg) and NASA Technical Report Server—Public (NTRS) thus providing one of the largest collections of aeronautical and space science STI in the world. Results are published in both non-NASA channels and by NASA in the NASA STI Report Series, which includes the following report types:

- TECHNICAL PUBLICATION. Reports of completed research or a major significant phase of research that present the results of NASA programs and include extensive data or theoretical analysis. Includes compilations of significant scientific and technical data and information deemed to be of continuing reference value. NASA counter-part of peer-reviewed formal professional papers, but has less stringent limitations on manuscript length and extent of graphic presentations.

- TECHNICAL MEMORANDUM. Scientific and technical findings that are preliminary or of specialized interest, e.g., "quick-release" reports, working papers, and bibliographies that contain minimal annotation. Does not contain extensive analysis.

- CONTRACTOR REPORT. Scientific and technical findings by NASA-sponsored contractors and grantees.

- CONFERENCE PUBLICATION. Collected papers from scientific and technical conferences, symposia, seminars, or other meetings sponsored or co-sponsored by NASA.

- SPECIAL PUBLICATION. Scientific, technical, or historical information from NASA programs, projects, and missions, often concerned with subjects having substantial public interest.

- TECHNICAL TRANSLATION. English-language translations of foreign scientific and technical material pertinent to NASA's mission.

For more information about the NASA STI program, see the following:

- Access the NASA STI program home page at http://www.sti.nasa.gov

- E-mail your question to help@sti.nasa.gov

- Fax your question to the NASA STI Information Desk at 757-864-6500

- Telephone the NASA STI Information Desk at 757-864-9658

- Write to:
  NASA STI Program
  Mail Stop 148
  NASA Langley Research Center
  Hampton, VA 23681-2199

NASA/TM-20210009633 AIAA–2016–4630

# Post-Test Inspection of NASA's Evolutionary Xenon Thruster Long-Duration Test Hardware: Discharge Chamber

*Rohit Shastry and George C. Soulas*
*Glenn Research Center, Cleveland, Ohio*

Prepared for the
52nd Joint Propulsion Conference
cosponsored by the AIAA, ASME, SAE, and ASEE
Salt Lake City, Utah, July 25–27, 2016

National Aeronautics and
Space Administration

Glenn Research Center
Cleveland, Ohio 44135

June 2021

## Acknowledgments

The authors would like to thank and acknowledge Kevin McCormick and Jim Sovey for their invaluable aid throughout the post-test inspection process. The authors would also like to thank and acknowledge Pete Bonacuse, Terry McCue, and Joy Buehler of the Analytical Science Group at GRC for their outstanding work involving generation of size distributions of the discharge chamber flakes, SEM imaging, and putting up with our sometimes unreasonable demands on the fidelity of results. This work was funded by the NEXT-C project, which is led by NASA GRC under NASA's Science Mission Directorate.

*Level of Review*: This material has been technically reviewed by technical management.

Available from

NASA STI Program
Mail Stop 148
NASA Langley Research Center
Hampton, VA 23681-2199

National Technical Information Service
5285 Port Royal Road
Springfield, VA 22161
703-605-6000

This report is available in electronic form at http://www.sti.nasa.gov/ and http://ntrs.nasa.gov/

# Post-Test Inspection of NASA's Evolutionary Xenon Thruster Long-Duration Test Hardware: Discharge Chamber

Rohit Shastry and George C. Soulas
National Aeronautics and Space Administration
Glenn Research Center
Cleveland, Ohio 44135

## Abstract

The NEXT Long-Duration Test is part of a comprehensive thruster service life assessment intended to demonstrate overall throughput capability, validate service life models, quantify wear rates as a function of time and operating condition, and identify any unknown life-limiting mechanisms. The test was voluntarily terminated in February 2014 after demonstrating 51,184 h of high-voltage operation, 918 kg of propellant throughput, and 35.5 MN-s of total impulse. The post-test inspection of the thruster hardware began shortly afterwards with a combination of non-destructive and destructive analysis techniques, and is presently nearing completion. This paper presents relevant results of the post-test inspection for the discharge chamber as well as other miscellaneous components such as the high-voltage propellant isolators and electrical cabling. Comparison of magnetic field measurements taken during pretest and post-test inspections indicate that the field strength did not degrade, consistent with performance data obtained during the test. Inspection of discharge chamber mesh samples show a deposition coating primarily composed of grid material that is approximately 15 μm in thickness. This thickness is well within the retention capability of the mesh and is therefore not expected to present any issues. Approximately 3.1 grams of deposition flakes were found at the bottom of the discharge chamber, composed primarily of grid material and carbon. Calculated size histograms of these flakes indicate that 99 percent have a maximum dimension of 200 μm or smaller, which is significantly less than the ion optics grid gap. Larger flakes that are capable of causing a grid-to-grid short will be analyzed to determine if their formation will occur in flight or is a facility effect. The high-voltage propellant isolators as well as numerous other electrical insulators were inspected and no evidence of arcing or any other issues were found.

### Nomenclature

| | |
|---|---|
| BSE | Backscattered Electron |
| EDS | Energy Dispersive x-ray Spectroscopy |
| ELT | Extended Life Test |
| GRC | Glenn Research Center |
| HVPI | High-Voltage Propellant Isolator |
| IPS | Ion Propulsion System |
| $J_B$ | beam current, A |
| LDT | Long-Duration Test |
| NEXT | NASA's Evolutionary Xenon Thruster |
| NEXT-C | NASA's Evolutionary Xenon Thruster - Commercial |
| NSTAR | NASA's Solar Electric Propulsion Technology Application Readiness |
| PPU | Power Processor Unit |
| QCM | Quartz Crystal Microbalance |
| SEM | Scanning Electron Microscopy |
| $V_B$ | beam power supply voltage, V |

# 1.0 Introduction

NASA has identified the need for a higher-power, higher-specific impulse, higher-thrust, and higher-throughput capable ion propulsion system (IPS) beyond the state-of-the-art NASA Solar Electric Propulsion Technology Application Readiness (NSTAR) IPS employed on the Deep Space 1 and Dawn Missions (Refs. 1 to 4). To fill this need, the NASA's Evolutionary Xenon Thruster (NEXT) IPS development, led by the NASA Glenn Research Center (GRC), was competitively selected in 2002. The NEXT IPS advanced technology was developed under the sponsorship of NASA's In-Space Propulsion Technology Program, with Phase 2 close-out of the NEXT IPS development occurring in 2012. The highest fidelity NEXT hardware planned was built by the government/industry NEXT team and includes: an engineering model (referred to as prototype model) thruster, an engineering model power processor unit (PPU), engineering model propellant management assemblies, a prototype gimbal, and control unit simulators (Ref. 5). Each of the units underwent extensive component-level testing, completed environmental testing (with the exception of the PPU), and was tested together in system integration testing (Refs. 6 to 9). Results from IPS component testing and integration testing can be found in References 7 to 17.

The NEXT thruster service life capability is being assessed through a comprehensive service life validation scheme that utilizes a combination of testing and analyses. Since the NEXT thruster is an evolution of the NSTAR thruster design, insights into the operation and erosion processes gained from NSTAR's development project apply to the NEXT thruster. The NEXT thruster, as a second-generation deep-space gridded ion thruster, made use of over 70,000 h of ground and flight test experience (not including the accumulated hours from the NSTAR IPS on the ongoing Dawn mission) in both the design of the NEXT thruster and evaluation of thruster wear-out failure modes. A NEXT service life assessment was conducted at NASA GRC, employing several models to evaluate all known failure modes with high confidence based upon the substantial amount of ion thruster testing dating back to the early 1960s (Refs. 18 to 19). The NEXT service life assessment also incorporated results from the NEXT 2,000 h wear test conducted on a NEXT laboratory model (referred to as engineering model) thruster operating at full power (6.9 kW) (Refs. 18 and 20). The transparency between the engineering model and prototype model thruster wear characteristics was demonstrated by a short-duration prototype model wear test (Refs. 21). The references for the NEXT service life assessment explain the thruster performance and erosion modeling analyses (Refs. 18 to 19).

The NEXT Long-Duration Test (LDT) was initiated in June 2005 as part of the comprehensive thruster service life assessment. The goals of the test were to demonstrate the initial project qualification propellant throughput requirement of 450 kg, validate the thruster service life model's predictions, quantify thruster performance and erosion as a function of thruster wear and throttle level, and identify any unknown life-limiting mechanisms. In December 2009, after successfully demonstrating the original qualification throughput requirement of 450 kg, the first listed goal was redefined to test to failure of the thruster or until decision to terminate the test voluntarily.

A decision to voluntarily terminate the test was made in April 2013 due to budget constraints. After a comprehensive end-of-test performance characterization was completed (Refs. 22), the thruster was vented to atmospheric conditions in April 2014. At the end of the test, the thruster had accumulated 51,184 h of high-voltage operation, processed 918 kg of xenon propellant, and delivered 35.5 MN-s of total impulse, setting numerous records for the most demonstrated lifetime of an electric propulsion device. Post-test inspection of the hardware was initiated soon after removal of the thruster from the vacuum facility. The results of this inspection for the discharge chamber as well as miscellaneous other

components are the subject of this paper. Results for other thruster components, including the ion optics and cathodes, and covered in companion publications (Refs. 23 to 24).

In April 2015, Aerojet Rocketdyne (with subcontractor ZIN Technologies) was competitively selected for the NASA's Evolutionary Xenon Thruster – Commercial (NEXT-C) contract. The objectives of this contract are two-fold: 1) To deliver two flight thrusters and two PPUs for use in future NASA missions, and 2) take steps to transition NEXT into a commercially available, off-the-shelf IPS for use by NASA as well as other interested parties. While the LDT was initiated as part of the Phase 2 effort under NASA's In-Space Propulsion Technology Program, the post-test inspection of the LDT thruster hardware has now fallen under the NEXT-C contract to be performed as an in-house task by GRC. The results of the LDT will then be relayed to Aerojet Rocketdyne along with any recommended design improvements to be made to the thruster flight design.

The paper is organized as follows: Section 2.0 covers the background for the NEXT LDT, including details of the test article as well as the throttling profile used over the course of the test. Section 3.0 describes the post-test inspection objectives, as well as the overall approach that was taken. Section 4.0 includes major results of the post-test inspection for the discharge chamber and miscellaneous components such as the propellant isolators, including resolution of issues encountered during the test. Section 5.0 then summarizes key findings and briefly describes remaining future work.

## 2.0 NEXT Long-Duration Test Background

The NEXT LDT was conducted within Vacuum Facility 16 at NASA GRC. The test article is a modified version of an engineering model (designated EM3), shown firing in Figure 1. To obtain a flight-representative configuration, prototype-model ion optics were incorporated, provided by industry partner Aerojet Corporation (now Aerojet Rocketdyne). A graphite discharge cathode keeper electrode was also incorporated into EM3 (Refs. 25). The NEXT thruster is nominally a 0.5 to 6.9 kW input power xenon thruster utilizing 2-grid dished-out ion optics, capable of producing thrust levels of 25 to 235 mN and specific impulses of 1400 to 4160 s. The technical approach for NEXT continues the derating philosophy used for the NSTAR ion thruster. A beam extraction area of 1.6X that of NSTAR allows for higher thruster input power while maintaining low discharge voltages and ion current densities, thus maintaining thruster longevity. Additional descriptions of the hardware, including the NEXT EM3 design and vacuum facility, can be found in References 2, 26, 27 to 31.

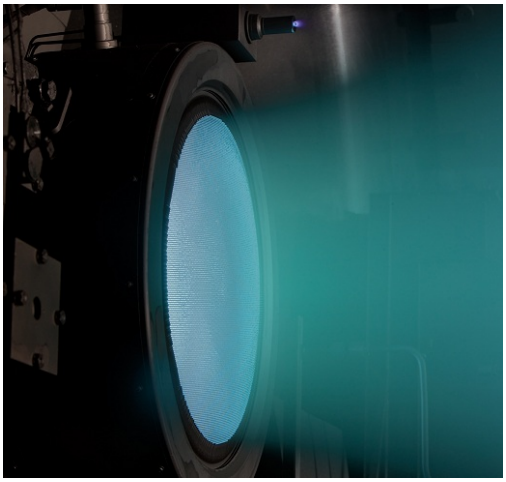

Figure 1.—Photograph of NEXT EM3 firing within Vacuum Facility 16 at GRC.

TABLE I.—NEXT LONG-DURATION TEST MISSION-REPRESENTATIVE THROTTLING PROFILE

| Throttle segment | Throttle level | Input power, kW | Operating condition ($J_B$, $V_B$) | Segment duration, kh | End of segment date |
|---|---|---|---|---|---|
| 1 | TL40 | 6.9 | 3.52 A, 1800 V | 13.0 | 11/17/2007 |
| 2 | TL37 | 4.7 | 3.52 A, 1179 V | 6.5 | 12/23/2008 |
| 3 | TL05 | 1.1 | 1.20 A, 679 V | 3.4 | 06/24/2009 |
| 4 | TL01 | 0.5 | 1.00 A, 275 V | 3.2 | 12/15/2009 |
| 5 | TL12 | 2.4 | 1.20 A, 1800 V | 3.1 | 05/05/2010 |
| 6 | TL40 | 6.9 | 3.52 A, 1800 V | 21.9 | 02/28/2014 |

Various diagnostics were utilized to characterize the performance and wear of the thruster during the LDT. These include: three staggered planar probes on a single-axis motion table to monitor ion current density distributions and beam divergence, a quartz crystal microbalance (QCM) to monitor backsputtered efflux from the facility, and an E × B probe to monitor the charge-state signature of the thruster plume. A data acquisition and control system was also used to monitor the thruster telemetry at 15 Hz and permit autonomous operation. A set of six in situ, charge-coupled device cameras were placed on the single-axis motion table to monitor wear rates of critical components on the thruster. These cameras imaged the downstream neutralizer keeper and cathode orifice plates, the discharge keeper and cathode orifice plates, accelerator grid apertures at various radials locations from centerline, and the cold grid gap of the ion optics. Additional details of the testing and facility diagnostics can be found in References 29 and 32.

The NEXT IPS was designed for solar electric propulsion applications that experience variable input power as the available solar flux changes with distance from the sun throughout the mission. For the LDT, the EM3 thruster was operated in a mission-representative profile comprised of discrete segments at various power levels shown in Table I and described in detail in Reference 33. The thruster was operated at each of these segments for sufficient duration to characterize the performance and wear rates, and to validate the thruster service life models. The throttle profile was completed in May 2010 and the thruster was then operated at full power until the end of the test in February 2014. For the majority of the test, detailed performance characterizations were carried out at 11 of the 40 operating conditions in the NEXT throttle table. These characterizations included overall thruster performance as well as component performance of the discharge chamber, neutralizer cathode, and ion optics. A comprehensive performance characterization was also performed at the end of the test that included all 40 operating conditions in the NEXT throttle table. Details of performance measurements as well as in situ images taken during the test can be found in References 22, 28, 29, 32 to 40.

## 3.0 Post-Test Inspection Objectives and Approach

The post-test inspection for the NEXT LDT largely followed the same approach and processes as what was employed for the inspection of the NSTAR Extended Life Test (ELT) thruster hardware (Ref. 41). The primary objectives of the post-test inspection are to: measure critical thruster wear rates that can induce thruster failure, to verify both in situ measurements and the service life model predictions; resolve any thruster-related issues encountered during the NEXT LDT; verify that thruster design changes made as a result of prior wear test findings had the desired impacts; and identify any unanticipated life-limiting phenomena. The thruster components were first inspected non-destructively in order to preserve the hardware for potential future testing. It was originally thought that resolution of issues encountered during the test or further characterization of the state of the hardware may require additional operation of

individual components or the thruster as a whole. However, after reviewing results from the non-destructive inspection, it was determined that resolution of many open issues and questions required destructive inspection of various thruster components.

Particular attention was paid to failure modes that were identified during the initial lifetime assessment and service life modeling for the NEXT thruster (Ref. 18). For the discharge chamber, these failure modes include: magnetic field degradation due to excessive temperatures; poor flake retention of sputtered material, from the thruster as well as the vacuum facility; and deposition of sputtered material on insulators, including within the high-voltage propellants isolators (HVPIs), which degrade their voltage standoff capability.

During thruster operation, the magnets placed within the discharge chamber will heat up due to proximity to the discharge plasma. These magnets were designed to withstand high temperatures; however, if much higher discharge currents are required as the thruster wears or if the chamber cannot reject heat as efficiently during its operational lifetime, overheating of the magnets may occur. This would result in magnetic field degradation, and thus reduce the discharge and overall thruster efficiencies. Thus, post-test inspection must check the magnetic field strength within the chamber for any signs of degradation.

Numerous thruster surfaces, such as the screen grid, accelerator grid, and discharge cathode, erode during thruster operation and deposit material on the inside surface of the discharge chamber. Deposition may also come from the vacuum facility as backsputtered material during ground testing. If these deposits build up and spall off, they could potentially cause an electrical short between the screen and accelerator grids. To prevent this from occurring, the discharge chamber is lined with a flake retention mesh. This mesh is designed to increase deposition adherence to the inside surface of the discharge chamber. Furthermore, if deposition does spall off, the mesh is designed to limit the size of the flakes so that they do not exceed the size of the grid gap and potentially cause a grid short. Thus, the post-test inspection of the hardware needed to verify that the flake retention mesh was successful and that any flakes within the discharge chamber were kept to an acceptable size that cannot cause grid shorts.

Propellant isolators are used to electrically isolate thruster components from the grounded flow lines further upstream. In particular, the HVPIs are placed in-line with the discharge cathode and main plenum flow lines, as these components will be at approximately 1800 V above facility ground at full power operation. During the post-test inspection, these components must be checked for any degradation or signs of arcing.

Apart from the tasks above, the post-test inspection of the hardware was needed to resolve a number of issues encountered during the test. For the discharge chamber in particular, the cause of an observed low impedance between the screen grid and the discharge anode (chamber) needed to be determined. Pertinent results from all these tasks are described in the following section.

# 4.0 Results and Discussion

## 4.1 Magnetic Field

Magnetic field strength was measured during the post-test inspection after the ion optics were removed. A full volumetric map within the discharge chamber was performed with a 3-axis gaussmeter, identical to what was used to measure the field during the pretest inspection. The field strength at centerline was then extracted from this map and compared to the pretest profile. Figure 2 shows the difference in field strength between pretest and post-test conditions along the discharge chamber centerline. For most of the discharge chamber, the measurements differ by less than 0.5 G, indicating little to no change in field strength. Differences approaching 5 to 6 G were found closer to the upstream surface

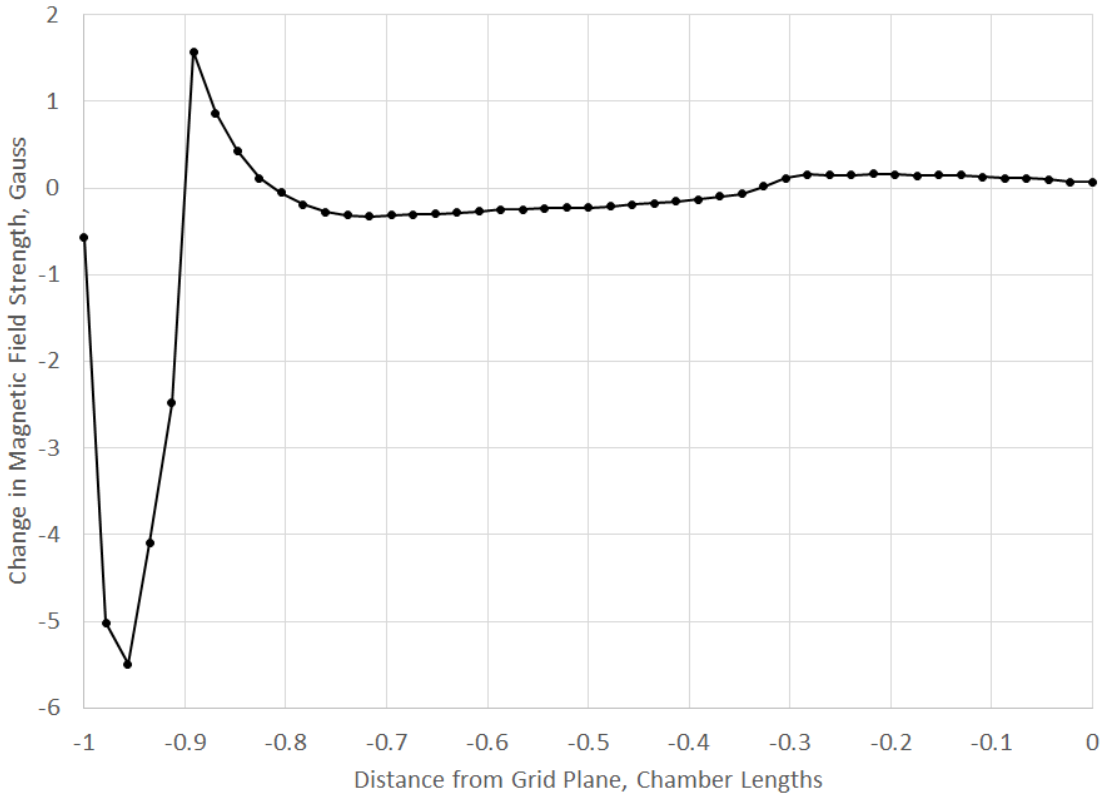


Figure 2.—Change in magnetic field strength between post-test and pretest measurements along the discharge chamber centerline.

of the chamber. It should be noted that this region is characterized not only by higher magnetic field strengths but also higher field gradients. Therefore, slight position uncertainties, especially with the presumed zero location, are likely responsible for the larger differences observed upstream. Analysis of the entire volumetric map indicates that the magnetic field had not degraded.

The magnetic field was also checked during post-test inspection by performing measurements at the surface of each magnet ring at several azimuthal locations. These measurements were also compared to similar pretest measurements to determine if magnetic field degradation had occurred. Unfortunately, this measurement was found to be highly sensitive to the exact location along the ring due to discrete magnet locations composing each ring, as well as the relative angle between the magnet and the 3-axis gaussmeter probe. During the post-test inspection, these factors were varied slightly in order to find the maximum field strength in the area, which yielded repeatable results. This technique was not used in the pretest inspection, making it very difficult to repeat for proper comparisons of the field strength. However, when comparing the measured maxima along each magnet ring, the pretest and post-test measurements agreed to within ± 6 percent, with the post-test value being the greater of the two most of the time. This offers further evidence that the magnetic field strength was not reduced due to overheating, which is consistent with discharge performance measured throughout the test (Ref. 22).

## 4.2 Discharge Chamber Mesh

In order to inspect the discharge chamber mesh, strips of the mesh were cut out of the discharge chamber and analyzed using scanning electron microscopy (SEM). Because the deposition on the mesh was assumed to be axisymmetric, these strips were removed at a single azimuthal location along the entire length of the discharge chamber. The azimuthal location was on the bottom half of the discharge chamber in an area that did not contain large amounts of discharge chamber flakes (see Section 4.3). Figure 3 shows backscattered electron (BSE) photomicrographs of the discharge chamber mesh sample that was closest to the ion optics. Elemental composition was determined using Energy Dispersive x-ray Spectroscopy (EDS). Under high magnification, a deposition coating was found on the wire mesh that was primarily composed of grid material. These results are qualitatively similar to what was observed in the NSTAR ELT hardware (Ref. 41). Within the coating, small flakes or nodules are also evident. While the majority of these nodules were composed of grid material, some had a high concentration of carbon that is most likely backsputtered material from the facility. It is also possible that some of the carbon had come from the discharge cathode keeper, which had exhibited erosion of the downstream face as well as the orifice (Ref. 23).

Samples of the discharge chamber mesh further upstream showed significantly more flakes that were lodged in between the wires of the mesh. Furthermore, numerous broken edges were observed within the deposition layer (see Figure 4). While it is possible that this is an indication of spalling from the surface, it is likely that the coating had fragmented during removal and subsequent handling of the sample. Regardless, these broken edges provide insight into the overall thickness and structure of the deposition on the mesh. Figure 4 shows an SEM image that indicates the deposition is composed of multiple layers, with lighter layers composed primarily of grid material while darker layers have a significant carbon component. The overall estimated deposition thickness based on this broken edge is approximately 15 μm. For comparison, the NSTAR ELT had a deposition thickness of approximately 10 μm near the ion optics (Ref. 41). This is well below the estimated maximum deposition thickness that can successfully adhere to the flake retention mesh. These preliminary measurements indicate that there should be no issues with the discharge chamber mesh retaining the deposition over the service life of the thruster. However, additional studies are planned that will section these mesh samples in order to better characterize the deposition thicknesses as a function of distance from the ion optics.

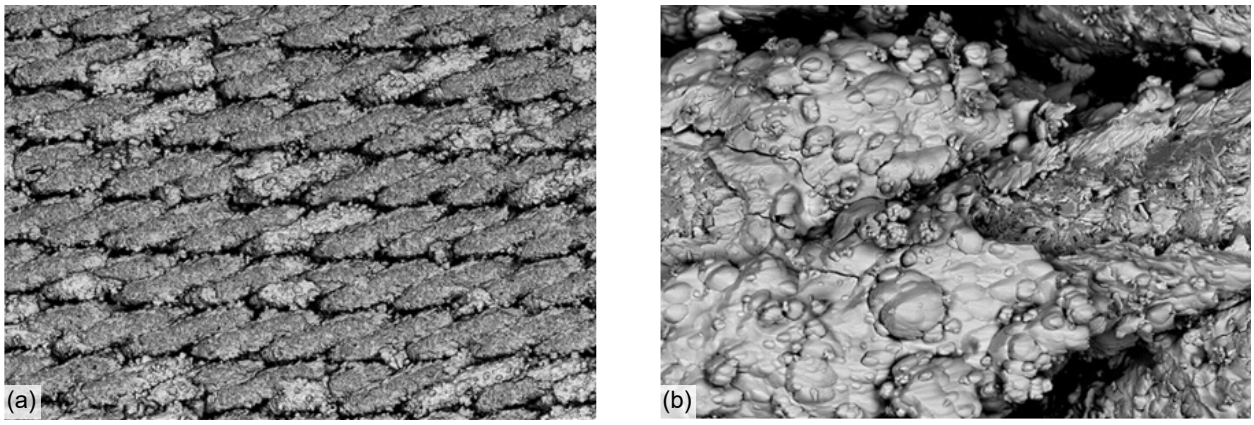


Figure 3.—Backscattered electron images of a discharge chamber mesh sample near the ion optics. (a) Low-magnification view, and (b) high-magnification view, illustrating the deposition coating on the wires.

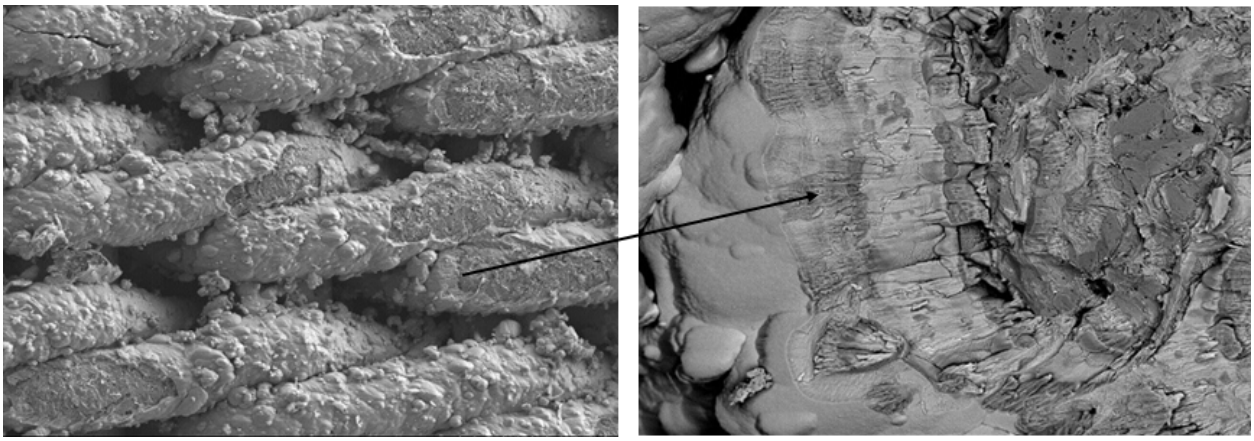

Figure 4.—Scanning electron microscopy images illustrating broken edges in the coating that give an indication of the deposition thickness and layered structure.

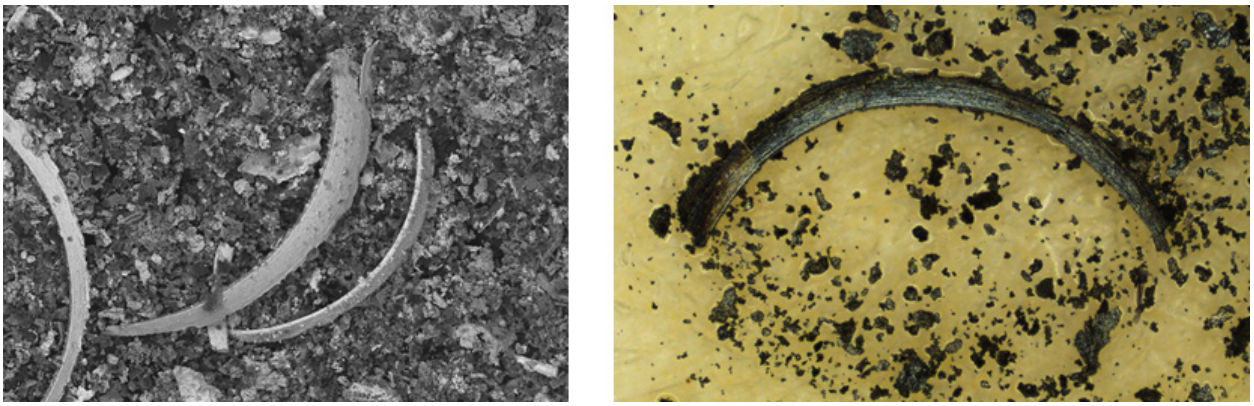

Figure 5.—Samples of discharge chamber flakes that exhibited a semi-circular shape. Given the radius of curvature of these flakes, they likely originated from the accelerator grid apertures.

## 4.3 Discharge Chamber Flakes

Inspection of the discharge chamber after the ion optics were removed revealed a large number of flakes present along the bottom of the cylindrical section of the chamber. This is similar to what was found in the NSTAR ELT, and was therefore expected (Ref. 41). These flakes were collected from discrete locations as well as general regions of the thruster, defined by axial distance from the ion optics. A total of 3.1 grams of material were collected from the bottom of the discharge chamber.

Samples of flakes from each region were visually inspected with an optical microscope. Many of the larger flakes found within the samples exhibited a semi-circular shape (see Figure 5). Based on the radius of curvature of these flakes, they likely had spalled from the apertures on the accelerator grid. The semi-circular flakes were found to be composed primarily of grid material, with some carbon content which was likely backsputtered material from the vacuum facility. Similar flakes were also found in the NSTAR ELT discharge chamber, also originating from the accelerator grid (Ref. 41).

In order to determine the likelihood of flakes being large enough to bridge the grid gap, optical images of the flake samples from each region were taken and analyzed to determine size distributions. Figure 6 provides analysis results for flake samples near the ion optics. These results show that 99 percent of the flakes within the sample have a maximum dimension less than 200 μm, which is significantly smaller than the grid gap of the thruster. Analysis of flakes from other regions further upstream yielded similar results. This indicates that the likelihood of flakes having dimensions large enough to bridge the grid gap

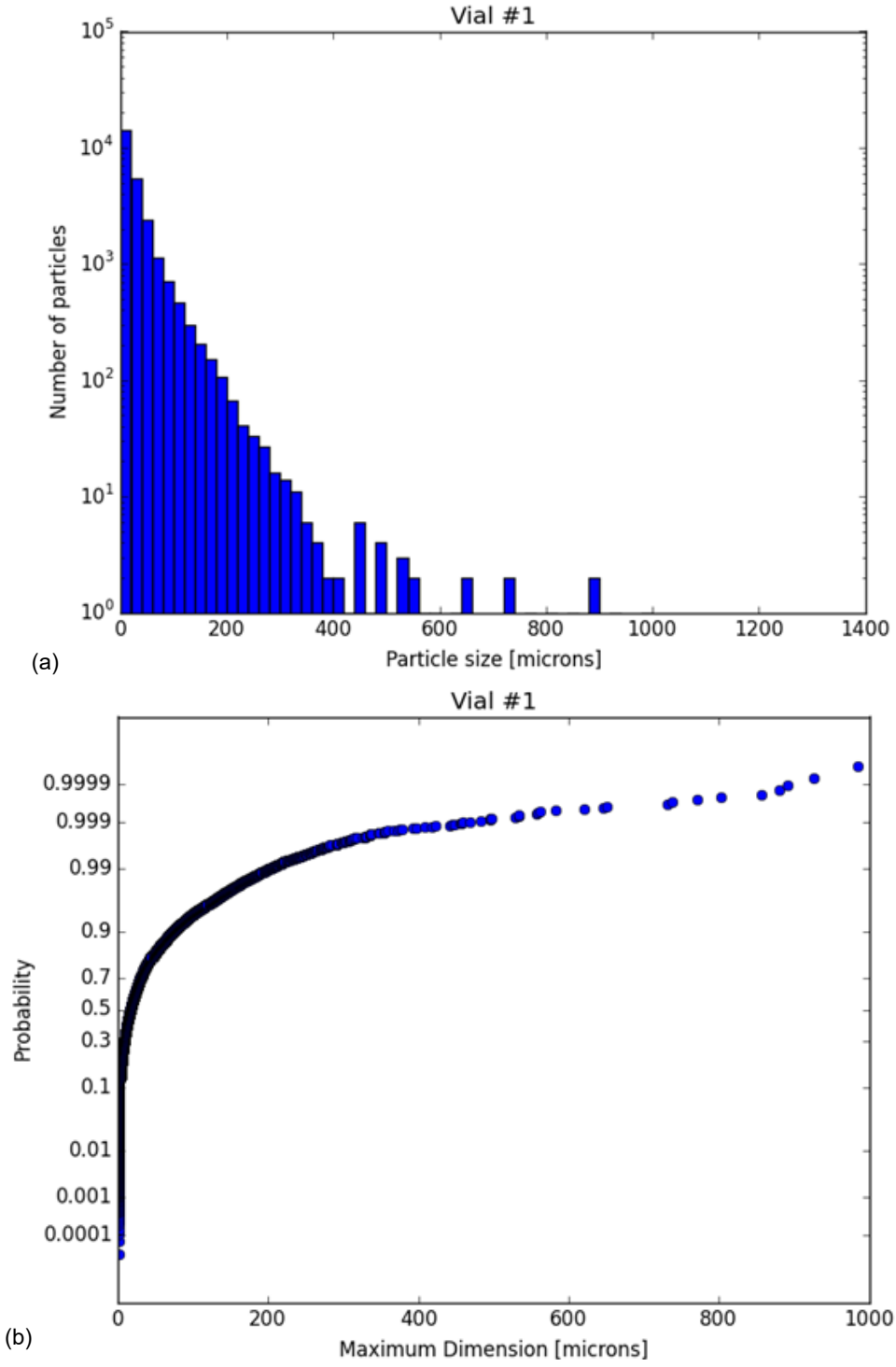


Figure 6.—Size distributions for the sample of flakes taken near the ion optics.
(a) Histogram of the size distribution based on the largest dimension of each flake.
(b) Probability that the flakes will be smaller than the specified dimension.

is relatively small. However, this analysis has also shown that flakes large enough to bridge the gap, while small in number, are present in the discharge chamber. Large flakes capable of causing a grid short were also found within the discharge chamber in the NSTAR ELT. For the ELT, elemental and structural analysis of several of these flakes revealed that many of them originated from the outside of the thruster, initially forming as backsputtered carbon deposition from the facility (Ref. 41). Thus it was concluded that such flakes would not form in a flight environment and therefore there was little risk in flakes causing a grid short. A similar analysis on the larger flakes found in the NEXT LDT is planned in order to determine their source and whether these flakes will form in flight.

## 4.4 High Voltage Propellant Isolators and Electrical Insulators

Prior to removal from the thruster, each HVPI was visually inspected, checked for flow leaks and had their impedances measured. A helium leak test of both HVPIs indicated that no flow leaks were present, and impedances of the discharge cathode and main HVPIs with 1800 V applied were 356 and 300 GΩ, respectively. This is not surprising as no impedance issues were encountered during the test between the anode/cathode and facility ground. The HVPIs were then more thoroughly inspected after removing them from the thruster. Figure 7 shows photographs of the discharge cathode HVPI after it was removed from the thruster. Overall, the HVPI appeared to be in very good condition. The HVPI on the main plenum line looked to be in similar condition. The only visual difference was some discoloration on the downstream end of the discharge cathode isolator (see Figure 7(b)). While it is unknown how this discoloration formed, it did not cause any issues. Each HVPI was then destructively disassembled and examined. All electrical insulators within both HVPIs appeared clean with no signs of arcing. Overall, each HVPI was found to be in excellent working condition with no issues.

A number of electrical insulators on the thruster were also visually inspected and had their impedances measured. These included the discharge cathode wiring insulators, the ion optics mounting insulators, the gimbal insulators, and the neutralizer cathode assembly mounting insulators. All of the insulators were found to be clean, with no signs of arcing. Furthermore, all impedances measured at maximum operating voltages were found to be 300 GΩ or higher. This indicated that all insulators are in excellent condition with no signs of degradation.

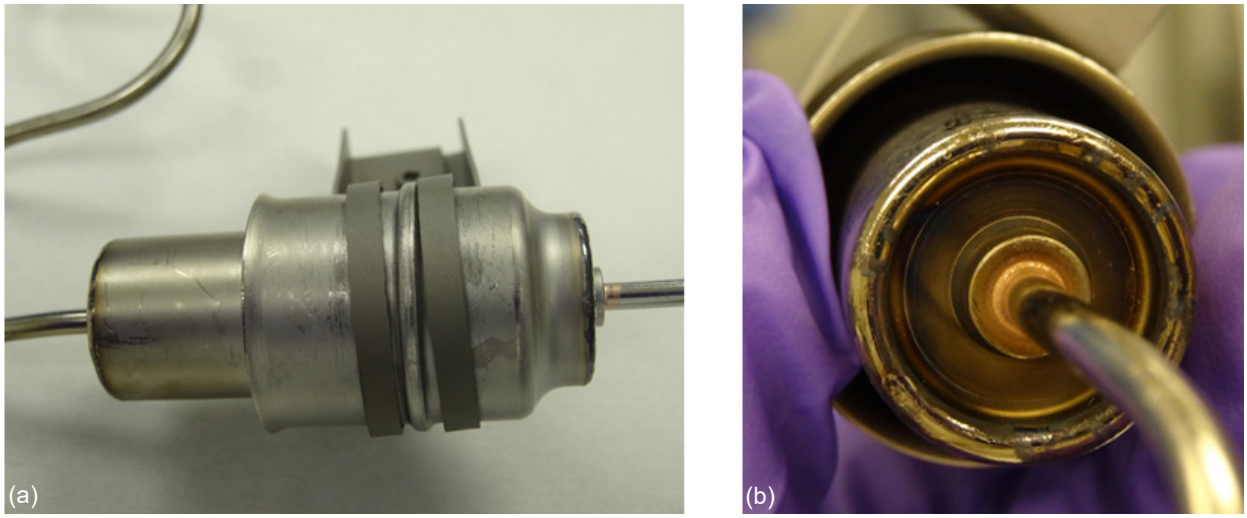


Figure 7.—Photographs of the discharge cathode HVPI after removal from the thruster. (a) Overall view of the isolator. Downstream side is on the left. (b) Face-on view of the downstream side, showing discoloration.

## 4.5 Electrical Cabling

A few impedance degradations were observed during the NEXT LDT. In particular, a low impedance developed between the anode and the screen grid. The impedance dropped off rapidly during the first 15 kh of operation, and was 40 to 50 kΩ at 45 V applied voltage by the end of the test. Because typical voltages between anode and the screen grid are limited to the discharge voltage (approximately 23 to 28 V), this impedance degradation did not cause any significant issues with thruster performance or lifetime. However, the cause still needed to be determined during the post-test inspection so that the degradation could potentially be avoided in future thruster builds.

In order to determine if there were any issues with the electrical lines, they were checked for breaks in the insulation as well as any signs of arcing. While a few locations on the anode and accelerator grid cables had nicks that exposed the inner layer of wire insulation, none of these areas were found to have lost proper electrical isolation from surfaces surrounding the wire. Furthermore, no signs of arcing were found along any of the electrical cabling.

While the majority of the cabling did not have any issues, deposition was found on the screen grid wire and insulating grommet as the wire passes through the anode from upstream of the discharge chamber to the screen grid (see Figure 8(a)). Resistance measurements were used to determine that this deposition was the cause of the low impedance between the screen grid and anode. Analysis using EDS revealed that the deposition is primarily composed of backsputtered carbon from the facility, indicating that this issue will not occur in flight. Additionally, the deposition material had likely passed through the perforated cylindrical plasma screen. Because the cylindrical plasma screen in the present flight thruster design is solid, this issue is also not expected to occur in future ground testing.

It is interesting to note that while the screen grid had reduced impedance to the anode due to backsputtered material passing through the plasma screen, the accelerator grid wire was only partially coated with deposition. Inspections revealed that a solid rib in the cylindrical plasma screen was properly positioned to shadow the accelerator grid wire and protect it from backsputtered carbon (see Figure 8(b)). Furthermore, the front mask of the thruster provided additional protection from deposition due to the accelerator grid wire terminal being further downstream than the screen grid wire terminal.

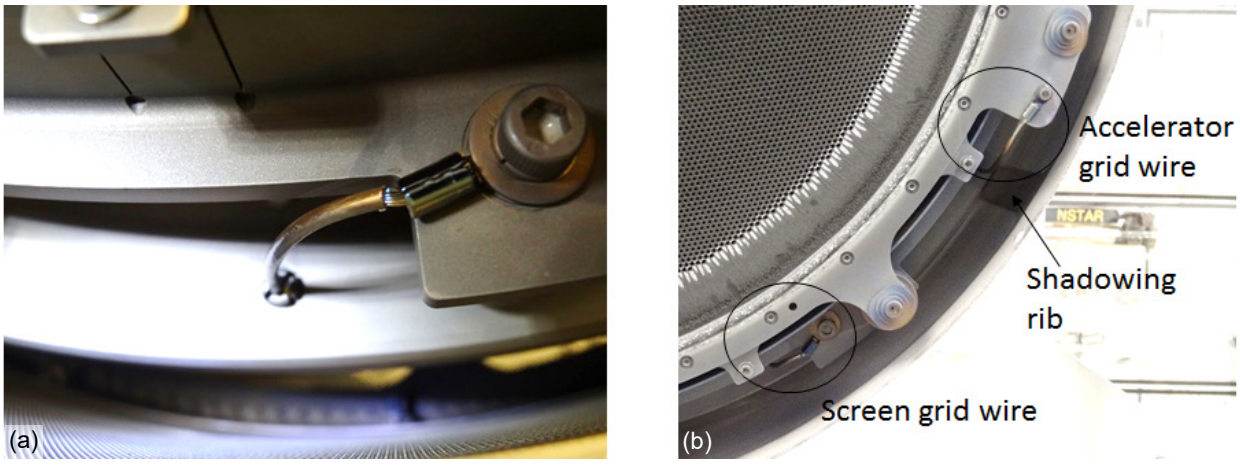


Figure 8.—Photographs of (a) deposition on the screen grid wire as it passes through the anode, and (b) the shadowing of the accelerator grid wire from deposition by a plasma screen rib.

## 5.0 Summary and Future Work

The NEXT LDT is part of a comprehensive thruster service life assessment intended to demonstrate overall throughput capability, validate service life models, quantify wear rates as a function of time and operating condition, and identify any unknown life-limiting mechanisms. In February 2014, the test was voluntarily terminated after demonstrating 51,184 h of high-voltage operation, 918 kg of propellant throughput, and 35.5 MN-s of total impulse. Post-test inspection began shortly afterwards and was focused on measuring critical thruster wear rates that can induce thruster failure to verify both in situ measurements and the service life model predictions, resolving any thruster-related issues encountered during the NEXT LDT, verifying that thruster design changes made as a result of prior wear test findings had the desired impacts, and identifying any unanticipated life-limiting phenomena. As of this publication, the post-test inspection is nearing completion and results with design improvements will be delivered to GRC's industry partner Aerojet Rocketdyne as they develop and build two NEXT flight thrusters and PPUs.

Measurements of the magnetic field strength within the discharge chamber volume as well as on the magnet ring surfaces indicate that the magnetic field has shown no degradation due to extended operation. Samples of the discharge chamber mesh were removed and analyzed to determine its effectiveness in retaining erosion products that deposit on the chamber surface. Preliminary findings indicate that the deposition had successfully adhered to the mesh with an overall thickness of approximately 15 μm, which is much less than the maximum thickness the mesh is capable of retaining. Numerous flakes were found at the bottom of the discharge chamber, similar to the ones found in the NSTAR ELT. The largest flakes exhibited a semi-circular shape and were determined to have likely spalled off of the accelerator grid apertures. Size distributions of the discharge chamber flakes indicate that approximately 99 percent of them have maximum dimensions of less than 200 μm, which is significantly smaller than the grid gap and are therefore not capable of causing a grid-to-grid short. The high-voltage propellant isolators as well as numerous other electrical insulators on the thruster were inspected. All insulators were found to be clean with no signs of arcing or any other issues. The electrical cabling was also determined to be free of damage and signs of arcing. However, deposition was found on the screen grid wire as it passes through the anode, resulting in the observed low impedance between these two components. This deposition was determined to be backsputtered carbon from the facility and is therefore not expected to occur in flight.

A few tasks remain to be completed for the post-test inspection of the discharge chamber. In particular, the mesh samples taken from the chamber must be sectioned in order to determine the deposition thickness as a function of axial distance from the ion optics. This will also allow for better characterization of the layering that was observed on the broken deposition edges. Additionally, the composition of discharge chamber flakes must be more thoroughly characterized to quantify the amount of flakes that originated from outside the thruster. This includes determining the composition and structure of larger flakes that may be the product of facility effects.

## References


1. Brophy, J. R., et al., "Development and Testing of the Dawn Ion Propulsion System," *42nd AIAA/ASME/SAE/ASEE Joint Propulsion Conference and Exhibit*, AIAA-2006-4319, Sacramento, CA, July 9-12, 2006.
2. Patterson, M. J. and Benson, S. W., "NEXT Ion Propulsion System Development Status and Performance," *43rd AIAA/ASME/SAE/ASEE Joint Propulsion Conference and Exhibit*, AIAA-2007-5199, Cincinnati, OH, July 8-11, 2007.

3. Polk, J. E., et al., "Demonstration of the NSTAR Ion Propulsion System on the Deep Space One Mission," *27th International Electric Propulsion Conference*, IEPC-2001-075, Pasadena, CA, October 15-19, 2001.
4. Rayman, M. D., "The Successful Conclusion of the Deep Space 1 Mission: Important Results Without a Flashy Title," *Space Technology*, Vol. 23, No. 2-3, 2003, pp. 185-196.
5. Benson, S. W. and Patterson, M. J., "NASA's Evolutionary Xenon Thruster (NEXT) Ion Propulsion Technology Development Status in 2009," *31st International Electric Propulsion Conference*, IEPC-2009-150, Ann Arbor, MI, September 20-24, 2009.
6. Hoskins, W. A., Aadland, R. S., Meckel, N. J., Talerico, L. A., and Monheiser, J. M., "NEXT Ion Propulsion System Production Readiness," *43rd AIAA/ASME/SAE/ASEE Joint Propulsion Conference and Exhibit*, AIAA-2007-5856, Cincinnati, OH, July 8-11, 2007.
7. Patterson, M. J., et al., "NEXT Multi-Thruster Array Test - Engineering Demonstration," *42nd AIAA/ASME/SAE/ASEE Joint Propulsion Conference and Exhibit*, AIAA-2006-5180, Sacramento, CA, July 9-12, 2006.
8. Snyder, J. S., Anderson, J. R., Van Noord, J. L., and Soulas, G. C., "Environmental Testing of the NEXT PM1 Ion Engine," *43rd AIAA/ASME/SAE/ASEE Joint Propulsion Conference and Exhibit*, AIAA-2007-5275, Cincinnati, OH, July 8-11, 2007.
9. Soulas, G. C., Patterson, M. J., Pinero, L., Herman, D. A., and Snyder, J. S., "NEXT Single String Integration Test Results," *45th AIAA/ASME/SAE/ASEE Joint Propulsion Conference and Exhibit*, AIAA-2009-4816, Denver, CO, August 2-5, 2009.
10. Aadland, R. S., Frederick, H., Benson, S. W., and Malone, S. P., "Development Results of the NEXT Propellant Management System," *JANNAF 2nd Liquid Propulsion Subcommittee and 1st Spacecraft Propulsion Subcommittee Joint Meeting*, JANNAF 2005-0356DW, Monterey, CA, December 5-8, 2005.
11. Crofton, M. W., et al., "Characterization of the NASA NEXT Thruster," *45th AIAA/ASME/SAE/ASEE Joint Propulsion Conference and Exhibit*, AIAA-2009-4815, Denver, CO, August 2-5, 2009.
12. Diamant, K. D., Pollard, J. E., Crofton, M. W., Patterson, M. J., and Soulas, G. C., "Thrust Stand Characterization of the NASA NEXT Thruster," *46th AIAA/ASME/SAE/ASEE Joint Propulsion Conference & Exhibit*, AIAA-2010-6701, Nashville, TN, July 25 - 28, 2010.
13. Herman, D. A., Pinero, L. R., and Sovey, J. S., "NASA's Evolutionary Xenon Thruster (NEXT) Component Verification Testing," *44th AIAA/ASME/SAE/ASEE Joint Propulsion Conference and Exhibit*, AIAA-2008-4812, Hartford, CT, July 21-23, 2008.
14. Herman, D. A., Soulas, G. C., and Patterson, M. J., "Performance Evaluation of the Prototype-Model NEXT Ion Thruster," *43rd AIAA/ASME/SAE/ASEE Joint Propulsion Conference and Exhibit*, AIAA-2007-5212, Cincinnati, OH, July 8-11, 2007.
15. Pinero, L. R., Hopson, M., Todd, P. C., and Wong, B., "Performance of the NEXT Engineering Model Power Processing Unit," *43rd AIAA/ASME/SAE/ASEE Joint Propulsion Conference and Exhibit*, AIAA-2007-5214, Cincinnati, OH, July 8-11, 2007.
16. Pollard, J. E., Diamant, K. D., Crofton, M. W., Patterson, M. J., and Soulas, G. C., "Spatially-Resolved Beam Current and Charge-State Distributions for the NEXT Ion Engine," *46th AIAA/ASME/SAE/ASEE Joint Propulsion Conference and Exhibit*, AIAA-2010-6779, Nashville, TN, July 25-28, 2010.
17. Snyder, J. S., et al., "Vibration Test of a Breadboard Gimbal for the NEXT Ion Engine," *42nd AIAA/ASME/SAE/ASEE Joint Propulsion Conference and Exhibit*, AIAA-2006-4665, Sacramento, CA, July 9-12, 2006.

18. Van Noord, J. L., "Lifetime Assessment of the NEXT Ion Thruster," *43rd AIAA/ASME/SAE/ASEE Joint Propulsion Conference and Exhibit*, AIAA-2007-5274, Cincinnati, OH, July 8-11, 2007.
19. Van Noord, J. L. and Herman, D. A., "Application of the NEXT Ion Thruster Lifetime Assessment to Thruster Throttling," *44th AIAA/ASME/SAE/ASEE Joint Propulsion Conference and Exhibit*, AIAA-2008-4526, Hartford, CT, July 21-23, 2008.
20. Soulas, G. C., Kamhawi, H., Patterson, M. J., Britton, M. A., and Frandina, M. M., "NEXT Ion Engine 2000 Hour Wear Test Results," *40th AIAA/ASME/SAE/ASEE Joint Propulsion Conference and Exhibit*, AIAA-2004-3791, Fort Lauderdale, FL, July 11-14, 2004.
21. Van Noord, J. L., Soulas, G. C., and Sovey, J. S., "NEXT PM1R Ion Thruster and Propellant Management System Wear Test Results," *31st International Electric Propulsion Conference*, IEPC-2009-163, Ann Arbor, MI, September 20-24, 2009.
22. Shastry, R., Herman, D. A., Soulas, G. C., and Patterson, M. J., "End-of-test Performance and Wear Characterization of NASA's Evolutionary Xenon Thruster (NEXT) Long-Duration Test," *50th AIAA/ASME/SAE/ASEE Joint Propulsion Conference*, AIAA-2014-3617, Cleveland, OH, July 28-30, 2014.
23. Shastry, R. and Soulas, G. C., "Post-test Inspection of NASA's Evolutionary Xenon Thruster Long-Duration Test Hardware: Discharge and Neutralizer Cathodes," *52nd AIAA/SAE/ASEE Joint Propulsion Conference*, Salt Lake City, UT, July 25 - 27, 2016 (to be published).
24. Soulas, G. C. and Shastry, R., "Post-test Inspection of NASA's Evolutionary Xenon Thruster Long Duration Test Hardware: Ion Optics," *52nd AIAA/SAE/ASEE Joint Propulsion Conference*, Salt Lake City, UT, July 25 - 27, 2016 (to be published).
25. Hoskins, W. A., et al., "Development of a Prototype Model Ion Thruster for the NEXT System," *40th AIAA/ASME/SAE/ASEE Joint Propulsion Conference and Exhibit*, AIAA-2004-4111, Fort Lauderdale, FL, July 11-14, 2004.
26. Soulas, G. C. and Patterson, M. J., "NEXT Ion Thruster Performance Dispersion Analyses," *43rd AIAA/ASME/SAE/ASEE Joint Propulsion Conference and Exhibit*, AIAA-2007-5213, Cincinnati, OH, July 8-11, 2007.
27. Frandina, M. M., Arrington, L. A., Soulas, G. C., Hickman, T. A., and Patterson, M. J., "Status of the NEXT Ion Thruster Long Duration Test," *41st AIAA/ASME/SAE/ASEE Joint Propulsion Conference and Exhibit*, AIAA-2005-4065, Tucson, AZ, July 10-13, 2005.
28. Herman, D. A., Soulas, G. C., and Patterson, M. J., "Performance Characteristics of the NEXT Long-Duration Test after 16,550 h and 337 kg of Xenon Processed," *44th AIAA/ASME/SAE/ASEE Joint Propulsion Conference and Exhibit*, AIAA-2008-4527, Hartford, CT, July 21-23, 2008.
29. Herman, D. A., Soulas, G. C., and Patterson, M. J., "NEXT Long-Duration Test Plume and Wear Characteristics after 16,550 h of Operation and 337 kg of Xenon Processed," *44th AIAA/ASME/SAE/ASEE Joint Propulsion Conference and Exhibit*, AIAA-2008-4919, Hartford, CT, July 21-23, 2008.
30. Patterson, M. J., et al., "NEXT: NASA's Evolutionary Xenon Thruster," *38th AIAA/ASME/SAE/ASEE Joint Propulsion Conference and Exhibit*, AIAA-2002-3832, Indianapolis, IN, July 7-10, 2002.
31. Soulas, G. C., Domonkos, M. T., and Patterson, M. J., "Performance Evaluation of the NEXT Ion Engine," *39th AIAA/ASME/SAE/ASEE Joint Propulsion Conference and Exhibit*, AIAA-2003-5278, Huntsville, AL, July 20-23, 2003.
32. Herman, D. A., Soulas, G. C., and Patterson, M. J., "Status of the NEXT Long-Duration Test after 23,300 Hours of Operation," *45th AIAA/ASME/SAE/ASEE Joint Propulsion Conference and Exhibit*, AIAA-2009-4917, Denver, CO, August 2-5, 2009.

33. Herman, D. A., “Status of the NASA's Evolutionary Xenon Thruster (NEXT) Long-Duration Test after 30,352 Hours of Operation,” *46th AIAA/ASME/SAE/ASEE Joint Propulsion Conference and Exhibit*, AIAA-2010-7112, Nashville, TN, July 25 - 28, 2010.
34. Herman, D. A., “NASA’s Evolutionary Xenon Thruster (NEXT) Project Qualification Propellant Throughput Milestone: Performance, Erosion, and Thruster Service Life Prediction after 450 kg,” *JANNAF 7th Modeling and Simulation, 5th Liquid Propulsion, and 4th Spacecraft Propulsion Joint Subcommittee Meeting*, CPIAC JSC 2010-0015EH and NASA TM-2010-216816, Colorado Springs, CO, May 3-7, 2010.
35. Herman, D. A., “Review of the NASA’s Evolutionary Xenon Thruster (NEXT) Long-Duration Test as of 632 kg of Propellant Throughput,” *47th AIAA/ASME/SAE/ASEE Joint Propulsion Conference and Exhibit*, AIAA-2011-5658, San Diego, CA, July 31 - August 3, 2011.
36. Herman, D. A., Soulas, G. C., and Patterson, M. J., “Status of the NEXT Ion Thruster Long-Duration Test after 10,100 h and 207 kg Demonstrated,” *43rd AIAA/ASME/SAE/ASEE Joint Propulsion Conference and Exhibit*, AIAA-2007-5272, Cincinnati, OH, July 8-11, 2007.
37. Herman, D. A., Soulas, G. C., and Patterson, M. J., “NEXT Long-Duration Test Neutralizer Performance and Erosion Characteristics,” *31st International Electric Propulsion Conference*, IEPC-2009-154, Ann Arbor, MI, September 20-24, 2009.
38. Herman, D. A., Soulas, G. C., Van Noord, J. L., and Patterson, M. J., “NASA’s Evolutionary Xenon Thruster Long-Duration Test Results,” *Journal of Propulsion and Power*, Vol. 28, No. 3, May - June, 2012, pp. 625-635.
39. Shastry, R., Herman, D. A., Soulas, G. C., and Patterson, M. J., “NASA's Evolutionary Xenon Thruster (NEXT) Long-Duration Test as of 736 kg of Propellant Throughput,” *48th AIAA/ASME/SAE/ASEE Joint Propulsion Conference and Exhibit*, AIAA-2012-4023, Atlanta, GA, July 29-August 1, 2012.
40. Shastry, R., Herman, D. A., Soulas, G. C., and Patterson, M. J., “Status of NASA’s Evolutionary Xenon Thruster (NEXT) Long-Duration Test as of 50,000 h and 900 kg Throughput,” *33rd International Electric Propulsion Conference*, IEPC-2013-121, Washington D.C., October 6-10, 2013.
41. Sengupta, A., et al., “The 30,000-Hour Extended-Life Test of the Deep Space 1 Flight Spare Ion Thruster,” NASA/TP—2004-213391, March, 2005.